Article

SOURCE DATA | TRANSPARENT PROCESS | OPEN ACCESS

THE EMBO JOURNAL

A conserved RNA seed-pairing domain directs small RNA-mediated stress resistance in enterobacteria

Nikolai Peschek[1,2], Mona Hoyos[1], Roman Herzog[1], Konrad U Förstner[3,4] & Kai Papenfort[1,2,*]

Abstract

Small regulatory RNAs (sRNAs) are crucial components of many stress response systems. The envelope stress response (ESR) of Gram-negative bacteria is a paradigm for sRNA-mediated stress management and involves, among other factors, the alternative sigma factor E (σ^E) and one or more sRNAs. In this study, we identified the MicV sRNA as a new member of the σ^E regulon in *Vibrio cholerae*. We show that MicV acts redundantly with another sRNA, VrrA, and that both sRNAs share a conserved seed-pairing domain allowing them to regulate multiple target mRNAs. *V. cholerae* lacking σ^E displayed increased sensitivity toward antimicrobials, and over-expression of either of the sRNAs suppressed this phenotype. Laboratory selection experiments using a library of synthetic sRNA regulators revealed that the seed-pairing domain of σ^E-dependent sRNAs is strongly enriched among sRNAs identified under membrane-damaging conditions and that repression of OmpA is crucial for sRNA-mediated stress relief. Together, our work shows that MicV and VrrA act as global regulators in the ESR of *V. cholerae* and provides evidence that bacterial sRNAs can be functionally annotated by their seed-pairing sequences.

Keywords Hfq; MicV; seed pairing; sigma E; sRNA

Subject Categories Microbiology, Virology & Host Pathogen Interaction; RNA Biology

DOI 10.15252/embj.2019101650 | Received 28 January 2019 | Revised 31 May 2019 | Accepted 9 June 2019 | Published online 17 July 2019

The EMBO Journal (2019) 38: e101650

Introduction

Regulatory RNAs are key factors for efficient gene expression control in all domains of life. It is now clear that RNA regulators can rival transcription factors with respect to their regulatory scope, as many regulatory RNAs control multiple and sometimes dozens of transcripts (Hor *et al*, 2018). Various RNA-sequencing-based technologies have led to the discovery of RNA regulators from almost all regions of the genome. However, while these approaches provided a great deal of information about the expression, conservation, and overall distribution of regulatory RNAs, they allowed only limited conclusions toward their physiological roles (Cruz & Westhof, 2009; Storz *et al*, 2011).

Regulatory RNAs have now been found by the hundreds in bacterial genomes (Sorek & Cossart, 2010). The largest and most thoroughly studied group of bacterial RNAs are called small regulatory RNAs (sRNAs) and frequently associate with the RNA chaperone Hfq (Kavita *et al*, 2018). Hfq belongs to the large family of RNA-binding Lsm/Sm-like proteins and is required for efficient stabilization and annealing of sRNAs to their transcript targets. In analogy to their miRNA (microRNA) and crRNA (CRISPR RNA) counterparts, the sRNAs recognize cognate targets by a short stretch of base-pairing nucleotides, called the "seed" sequence (Gorski *et al*, 2017). Seed sequences are ~6–12 nucleotides long and structurally accessible. Hfq-dependent sRNAs of γ-proteobacteria have been reported to carry up to three seed-pairing domains, and mutation of either of these domains results in loss of regulation for a subset of target mRNAs (Herzog *et al*, 2019). Initial base-pairing by the seed typically relies on Watson–Crick base-pairing; however, it is not fully understood how these interactions discriminate against off-target interactions involving non-canonical G-U base-pairs (Papenfort *et al*, 2012).

Several sRNAs have been investigated for their seed-pairing capacities (Gorski *et al*, 2017). Here, the RybB sRNA, controlling envelope homeostasis of Gram-negative bacteria, has emerged as a model to study the mechanisms underlying seed-pairing regulatory RNAs (Bouvier *et al*, 2008; Balbontin *et al*, 2010; Papenfort *et al*, 2010). Transcription of RybB is controlled by the alternative sigma factor σ^E (encoded by the *rpoE* gene; Johansen *et al*, 2006; Papenfort *et al*, 2006; Thompson *et al*, 2007). σ^E belongs to the large class of extracytoplasmic function σ factors (ECFs), which are negatively controlled by a corresponding anti-sigma factor (Sineva *et al*, 2017). Under regular growth conditions, σ^E activity is weak as the protein is tethered to the inner membrane-bound anti-sigma factor, RseA. Misfolded outer membrane proteins (OMPs) trigger a cascade of regulated proteolysis events degrading RseA and releasing σ^E into the cytoplasm. σ^E associates with the core RNA polymerase and directs transcription toward specific promoters. Besides RybB, σ^E activates ~100 genes in *Escherichia coli* and related bacteria (Rhodius *et al*, 2006), including two additional Hfq-dependent

1 Faculty of Biology I, Department of Microbiology, Ludwig-Maximilians-University of Munich, Martinsried, Germany
2 Munich Center for Integrated Protein Science (CIPSM), Munich, Germany
3 Institute of Information Science, TH Köln – University of Applied Sciences, Cologne, Germany
4 ZB MED – Information Centre for Life Sciences, Cologne, Germany
*Corresponding author. Tel: +49 8921 8074502; E-mail: kai.papenfort@lmu.de

sRNAs, MicA and MicL. RybB and MicA regulate multiple target mRNAs in response to activation of σ^E. Targets of MicA and RybB are enriched for mRNAs encoding OMPs, suggesting that the sRNAs function to reduce the production of newly synthesized OMPs when the outer membrane is damaged (Brosse & Guillier, 2018). In contrast, MicL acts to inhibit translation of the highly abundant Lpp protein, which tethers the outer membrane to the peptidoglycan layer (Guo *et al*, 2014). Given that σ^E-bound RNA polymerase is restricted to act as a transcriptional activator, the σ^E-activated sRNAs have been suggested to provide an important inhibitory function to the system (Gogol *et al*, 2011).

σ^E-dependent sRNAs have also been described in other organisms. For example, in the major human pathogen *Vibrio cholerae*, the VrrA sRNA is activated by σ^E and inhibits the expression of four mRNA targets: the transcripts of the major OMPs, OmpA and OmpT; the biofilm matrix protein, RbmC; and the ribosome hibernation protein, Vrp (Song *et al*, 2008, 2010, 2014; Sabharwal *et al*, 2015). VrrA has also been shown to promote the production of outer membrane vesicles and to modulate virulence (Song *et al*, 2008).

In this study, we harnessed transcriptomic data to search for σ^E-dependent genes in *V. cholerae*. Our analysis identified the MicV sRNA as a new member of the σ^E regulon and we show that MicV associates with Hfq to regulate multiple target transcripts, including several mRNAs encoding OMPs. Global identification of target mRNAs revealed that MicV and VrrA control at least 32 mRNAs. While each sRNA controls a set of specific transcripts, the majority of targets are shared by the two sRNAs. We discovered that a conserved seed-pairing sequence present in MicV and VrrA accounts for the overlapping target regulation and that combined mutation of *micV* and *vrrA* impairs survival of *V. cholerae* under membrane-damaging conditions. This phenotype can be overcome by overexpression of MicV, VrrA, or RybB from *E. coli*, which also carries the conserved seed-pairing sequence of σ^E-dependent sRNAs. By employing an sRNA library carrying randomized base-pairing sequences, we show that the seed-pairing domain of σ^E-dependent sRNAs is strongly enriched during laboratory selection experiments and high-throughput sequencing of the selected seed sequences revealed a strong prevalence for sRNAs capable of repressing the OmpA protein. Indeed, deletion of *ompA* efficiently alleviated stress sensitivity of *rpoE*-deficient *V. cholerae*. Our data highlight the crucial role of seed-pairing domains in regulatory RNAs and describe a novel sRNA-based approach to study complex bacterial phenotypes in an unbiased fashion.

Results

MicV is a σ^E-dependent sRNA

We have recently determined the transcriptomes of *V. cholerae* under conditions of low and high cell densities and identified a total of 7,240 transcriptional start sites (TSS; Papenfort *et al*, 2015). However, these analyses did not provide information on how the activities of these TSS are controlled and which sigma factors could be involved. To address this question, we used a bioinformatics approach and searched for the σ^E consensus motif upstream of the 7,240 TSS in *V. cholerae*. We discovered 73 TSS associated with the σ^E motif (Appendix Table S1), including several TSS of genes previously linked with σ^E. For example, the 73 TSS included the promoters for *lptD*, *rpoH*, and *rpoE* itself, which have been documented to be activated by σ^E in *E. coli* (Rhodius *et al*, 2006), as well as the promoter for the VrrA sRNA. Thus, our approach allows the identification of σ^E-controlled genes in *V. cholerae*.

In addition to VrrA, we discovered that the promoter of another 68-nucleotide sRNA, Vcr089 (Papenfort *et al*, 2015), carried a sequence that aligned with the σ^E consensus (Fig 1A). The *vcr089* sRNA is conserved among *Vibrios* (Fig 1A). In analogy to the σ^E-dependent MicA sRNA (Udekwu *et al*, 2005), we renamed this sRNA MicV. In *V. cholerae*, the *micV* gene is located in the intergenic region of the *vc2640* (encoding a hypothetical protein) and *vc2641* (encoding argininosuccinate lyase) genes (Fig EV1A). Northern blot analysis showed that MicV expression peaks in stationary phase and that two MicV isoforms can be detected: the full-length transcript and a processed shorter variant (Fig EV1B). A similar expression pattern is observed for the VrrA sRNA (Fig EV1B). We also recovered both MicV isoforms in Hfq co-immunoprecipitation experiments (Fig EV1C), and MicV stability was strongly reduced in *hfq*-deficient *V. cholerae* (Fig EV1D) showing that MicV is a Hfq-dependent sRNA. For comparison, VrrA stability was only mildly affected in cells lacking *hfq* (Fig EV1D).

To test whether *micV* is controlled by σ^E, we generated an *rpoE* deletion mutant in *V. cholerae*. The *rpoE* gene is considered essential in *V. cholerae* and to avoid unpredictable suppressor mutations, we first deleted the *vchM* gene, encoding a known suppressor of σ^E (Chao *et al*, 2015), followed by deletion of *rpoE*. The *vchM* deletion did not affect the expression of MicV or VrrA (Fig EV1B). Northern blot analysis of MicV and VrrA showed that both sRNAs are undetectable in cells lacking *vchM* and *rpoE* (from here on referred to as Δ*rpoE*), whereas plasmid-borne production of σ^E from the inducible P_{BAD} promoter strongly activated the expression of both sRNAs (Fig 1B). To compare MicV and VrrA expression detected by Northern blot analysis with the activity of their associated promoters, we generated mKate2-based transcriptional reporters for both sRNAs and monitored production of the fluorescent protein at various points in growth. In wild-type *V. cholerae*, activity of the *micV* promoter was weak in exponentially growing cells and strongly increased when cells entered stationary phase growth (Fig 1C). Comparable levels were found for the P*vrrA*::mKate2 reporter (Fig EV1E). Mutation of *vchM* did not have a significant effect on the performance of both reporters; however, mKate2 production was hardly detectable in Δ*rpoE* cells (Figs 1C and EV1E). Given the conserved role of σ^E in enterobacteria, we also monitored the activity of P*micV*::GFP in wild-type and Δ*rpoE E. coli*. Again, GFP production in wild-type cells reached a maximum in stationary phase growth, whereas promoter activity was strongly reduced in *rpoE*-deficient cells (Fig EV1F). P_{BAD}-driven production of *V. cholerae* and *E. coli* σ^E rescued and further elevated GFP production in *E. coli*, indicating that the *micV* promoter is recognized and activated by σ^E.

VrrA is required for ethanol resistance in *Vibrio cholerae*

Exposure to ethanol has been reported to induce σ^E-mediated gene expression in *V. cholerae* (Chatterjee & Chowdhury, 2013). To test the effect of ethanol on *vrrA* and *micV* expression, we cultivated wild-type and Δ*rpoE V. cholerae* carrying the P*micV*::mKate2 or

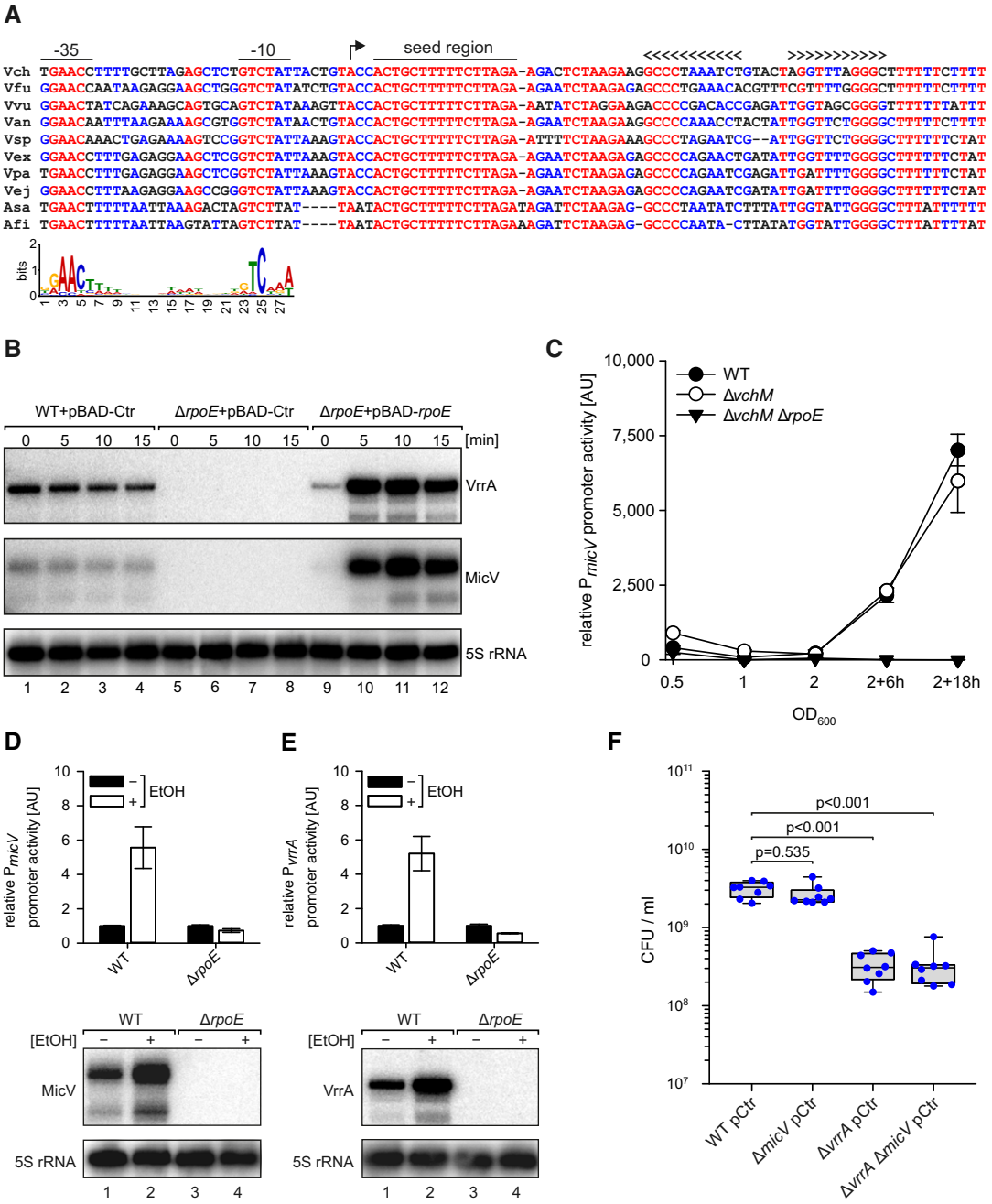

Figure 1. Transcriptional regulation of *micV*.

A Alignment of *micV* sequences, including the promoter regions, from various *Vibrio* species. The -35 box, -10 box, the TSS, the highly conserved seed region, and the rho-independent terminator are indicated. Lower part: consensus motif of *E. coli* σ^E-dependent promoters.

B *Vibrio cholerae* wild-type and Δ*rpoE* strains carrying the indicated plasmids were grown in LB medium to early stationary phase (OD_{600} of 1.5) and induced with L-arabinose (0.2% final conc.). Expression of MicV and VrrA was monitored on Northern blots. 5S rRNA served as loading control.

C *Vibrio cholerae* wild-type, Δ*vchM*, and Δ*vchM* Δ*rpoE* strains harboring the P*micV*::*mKate2* plasmid were grown in M9 minimal medium. Samples were collected at various stages of growth and analyzed for fluorescence.

D, E *Vibrio cholerae* wild-type and Δ*rpoE* strains carrying P*micV*::*mKate2* (D) or P*vrrA*::*mKate2* (E) plasmids were cultivated in LB medium to exponential phase (OD_{600} of 0.4) and treated with ethanol (3.5% final conc.) or water. Fluorescence was determined 180 min after ethanol treatment, and mKate2 levels of the mock-treated samples were set to 1. Corresponding Northern blot analyses of MicV and VrrA expression are shown at the bottom. 5S rRNA served as loading control.

F *Vibrio cholerae* wild-type, Δ*micV*, Δ*vrrA*, or Δ*vrrA* Δ*micV* strains were grown in LB medium to OD_{600} of 0.2 and treated with ethanol (3.5% final conc.). After 5 h of treatment, serial dilutions were prepared, recovered on agar plates, and CFU/ml were determined.

Data information: In (C–E), data are presented as mean ± SD, $n = 3$. In (F), the box plots indicate the median, 75th and 25th percentiles (boxes), and 90th and 10th percentiles (whiskers), $n = 8$. Statistical significance was determined using one-way ANOVA and post hoc Holm–Sidak test.
Source data are available online for this figure.

P*vrrA*::mKate2 reporters to exponential phase (OD_{600} of 0.4) and treated cells with ethanol (3.5% final conc.). After 180 min of exposure, we detected ~5-fold elevated mKate2 levels from the *micV* and *vrrA* promoters in wild-type cells, which we also confirmed at the transcript levels using Northern blot analysis (Fig 1D and E). In contrast, *rpoE*-deficient *V. cholerae* failed to significantly activate VrrA and MicV expression.

These results motivated us to investigate the role of *micV* and *vrrA* in *V. cholerae* challenged with ethanol. To this end, we treated exponential cultures (OD_{600} of 0.2) of wild-type, Δ*micV*, Δ*vrrA*, and Δ*vrrA* Δ*micV V. cholerae* with ethanol (3.5% final conc.) and determined CFU (colony forming units) after 5 h of incubation. While we discovered no significant difference in CFU for wild-type and Δ*micV V. cholerae*, Δ*vrrA* and Δ*vrrA* Δ*micV* cells displayed ~10-fold reduced CFU, when compared to the other two strains (Fig 1F). These data show that *micV* and *vrrA* are activated in response to membrane perturbations in *V. cholerae*, but only VrrA confers ethanol resistance.

MicV inhibits OmpT protein production

To study the role of MicV in gene regulation in *V. cholerae*, we constructed a MicV over-expression plasmid (pMicV) from which MicV production is driven by the constitutive P_{Tac} promoter. We transformed this plasmid into *V. cholerae* lacking *micV* and compared global changes in protein expression with wild-type and Δ*micV V. cholerae* carrying a control plasmid (pCtr) using SDS–PAGE (Appendix Fig S1A). Our data showed increased levels of a ~40 kDa protein in Δ*micV* cells and repression of the same protein when MicV was over-expressed (Appendix Fig S1A, compare lanes 3, 4 vs. 7, 8 vs. 11, 12). We excised the band from the gel and identified the protein as OmpT (VC1854) by mass spectrometry.

These data indicated that MicV inhibits OmpT expression in *V. cholerae*, as was also previously reported for the VrrA sRNA (Song *et al*, 2010). Given that both sRNAs are controlled by σ^E (Fig 1 and Song *et al*, 2008), we aimed to determine the contribution of each of the sRNAs to OmpT repression. To this end, we added a 3XFLAG epitope to the chromosomal *ompT* locus and monitored OmpT protein expression in wild-type, Δ*vrrA*, Δ*micV*, and Δ*vrrA* Δ*micV V. cholerae* at several stages of growth (Appendix Fig S1B, top). In accordance with the data presented in Appendix Fig S1A, OmpT production increased under stationary phase growth conditions and was elevated up to ~6-fold in cells lacking *micV*, when compared to wild-type *V. cholerae* (Appendix Fig S1B, lanes 1 vs. 3, 5 vs. 7, 9 vs. 11, and 13 vs. 15). OmpT was over-produced in Δ*micV* cells under all tested growth conditions (~6-fold at OD_{600} of 0.5 and 1.0, ~2.5-fold under stationary phase conditions), whereas lack of *vrrA* did not increase OmpT levels (lanes 2, 6, 10, and 14). However, mutation of both sRNAs (lanes 4, 8, 12, and 16) revealed an additive effect of the two sRNAs resulting in more than 12-fold higher OmpT levels when cells were cultivated to late exponential phase (OD_{600} of 1.0). Together, these results show that both MicV and VrrA repress OmpT production in *V. cholerae* with MicV being the dominant regulator under the tested conditions.

Over-production of OMPs has previously been reported to increase σ^E activity (Mecsas *et al*, 1993). Consequently, we predicted that elevated OmpT levels produced in Δ*micV* and Δ*vrrA* Δ*micV* cells would also increase σ^E activity in *V. cholerae*. To test this hypothesis, we collected total RNA samples using our previous experimental setup (Appendix Fig S1B) and probed VrrA and MicV levels on Northern blots. Indeed, we discovered increased VrrA accumulation in cells lacking *micV*, while mutation of *vrrA* had only a minor effect on *micV* expression (Appendix Fig S1B, bottom). In accordance with the hypothesis that increased OmpT production activates the ESR in *V. cholerae*, VrrA production was highest when OmpT levels were most strongly induced (~6-fold) in the *micV* mutant (Appendix Fig S1B, bottom, lanes 5 vs. 7). To corroborate these data with the status of the σ^E response, we used the P*micV*::mKate2 reporter as a proxy for σ^E activation in wild-type, Δ*vrrA*, Δ*micV*, and Δ*vrrA* Δ*micV V. cholerae* at several stages of growth (Appendix Fig S1C). When compared to wild-type *V. cholerae*, mKate2 levels did not change significantly in the *vrrA* mutant and were moderately induced in cells lacking *micV* (~1.5-fold). In contrast, mutation of both sRNAs had an additive effect on the activity of the *micV* promoter (~ 2.5-fold), suggesting that MicV and VrrA act redundantly to control σ^E activation in *V. cholerae*.

Global target profiles of MicV and VrrA in *Vibrio cholerae*

The VrrA sRNA has previously been shown to regulate multiple mRNAs through direct base-pairing, including *ompT* (Song *et al*, 2010). Likewise, we suspected that MicV inhibits *ompT* at the post-transcriptional level through translation repression and transcript degradation. To test whether MicV-mediated repression of *ompT* involves transcript degradation, we constructed an L-arabinose-inducible pBAD-*micV* plasmid. To avoid cross-regulation from chromosomal MicV and VrrA production, we transferred this plasmid into a *V. cholerae* mutant lacking *vrrA* and *micV* and investigated *ompT* levels by Northern blot analysis. Indeed, induction of MicV from this plasmid resulted in a rapid reduction of *ompT* mRNA (Fig 2A, lanes 3–7), whereas L-arabinose did not affect *ompT* levels in the same strain carrying a control vector (lanes 1–2). Moreover, the dynamics of MicV-mediated *ompT* repression were comparable to an equivalent experiment using a pBAD-*vrrA* plasmid (lanes 8–12), indicating that both sRNAs act post-transcriptionally on *ompT*.

These observations prompted us to design an experimental setup for the identification of MicV and VrrA target mRNA candidates at a genome-wide level. To this end, we cultivated Δ*vrrA* Δ*micV V. cholerae* carrying either pBAD-*micV*, pBAD-*vrrA*, or a control plasmid to early stationary phase (OD_{600} of 1.5) and induced sRNA expression from the P_{BAD} promoter for 10 min. Differentially expressed genes were determined by RNA-sequencing comparing cells induced for MicV or VrrA to the empty vector control. Transcripts displaying ≥ 3-fold change in abundance by either of the two sRNAs were considered potential target mRNAs. In total, we discovered 28 and 27 differently regulated genes for MicV and VrrA, respectively (Appendix Table S2 and Appendix Fig S2). Importantly, 23 of these targets, including *ompT*, were regulated by both sRNAs (Fig 2B).

Next, we tested whether the newly identified targets are regulated at the post-transcriptional level by MicV and/or VrrA. Specifically, we employed a well-established GFP-based reporter system tailored to determine post-transcriptional gene control in bacteria (Corcoran *et al*, 2012). In this system, the 5′ UTR (untranslated region) and the sequence corresponding to the first 20 amino acids of the target genes were fused to *gfp* under the control of the P_{TetO} promoter. These plasmids were transferred into *V. cholerae* along

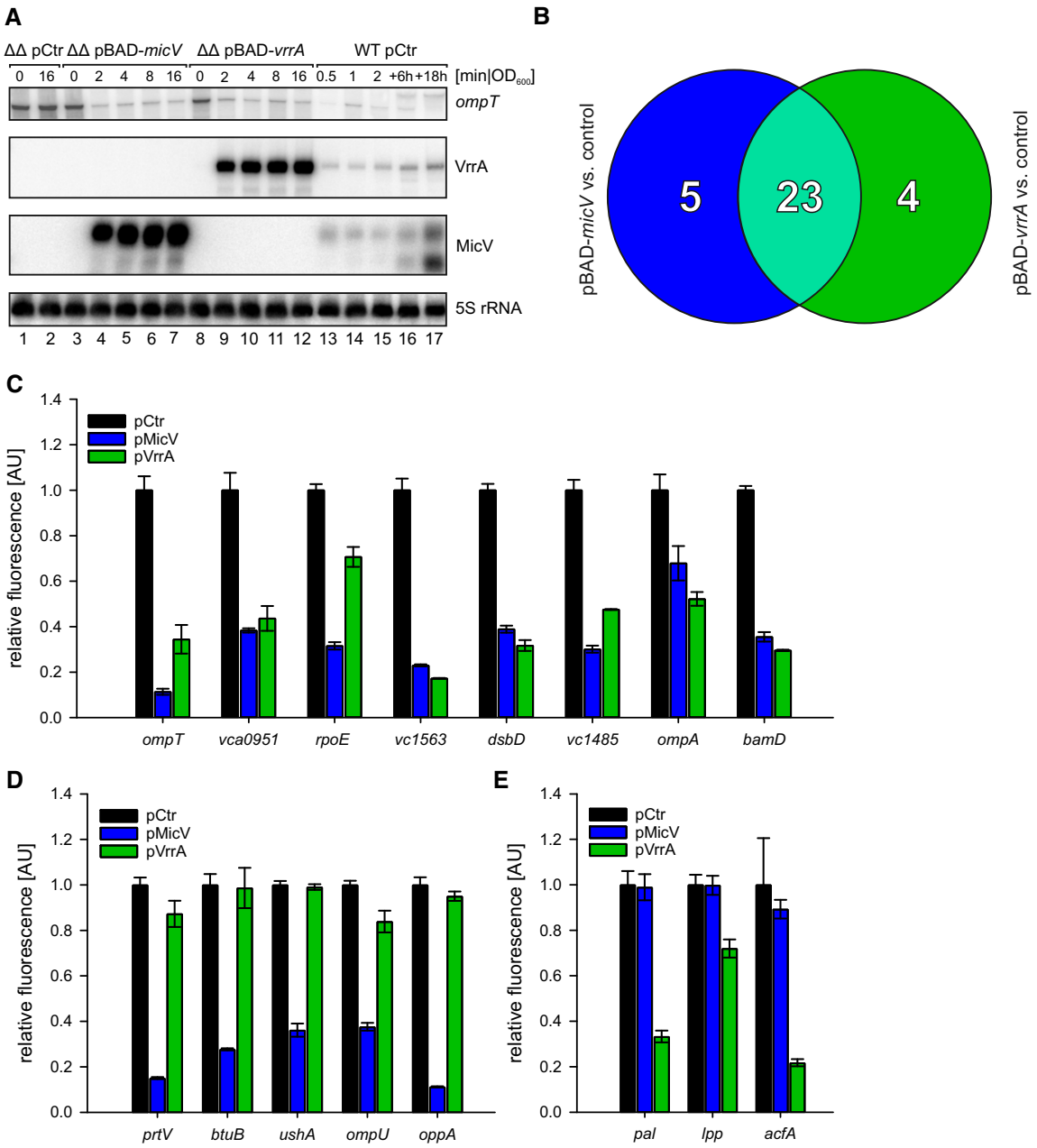

Figure 2. Target profiles of MicV and VrrA.

A *Vibrio cholerae* Δ*vrrA* Δ*micV* strains carrying pBAD-*micV*, pBAD-*vrrA*, or an empty vector control (pCtr) were cultivated to early stationary phase (OD_{600} of 1.5) in LB medium. Cells were treated with L-arabinose (0.2% final conc.), and RNA samples were collected at the indicated time points after induction. Northern blot analysis was performed to determine VrrA, MicV, and *ompT* levels. 5S rRNA served as loading control. For comparison, RNA samples of a wild-type strain carrying pCtr were collected during various growth phases, which indicated ~18-fold and ~7-fold higher levels of VrrA and MicV expressed from the pBAD plasmids, respectively (see Source data for quantifications).

B Venn diagram summarizing the RNA-Seq results: RNA samples were collected from *V. cholerae* Δ*vrrA* Δ*micV* strains carrying pBAD-*micV*, pBAD-*vrrA*, or an empty vector control. Depicted are genes displaying a fold change of ≥ 3 and FDR-adjusted p-value ≤ 1E-8 obtained from MicV-expressing conditions (blue) or *vrrA*-expressing conditions (green). Genes regulated by both sRNAs (fold change ≥ 3 in one condition, fold change ≥ 2.0 in the other) are depicted in light green.

C–E *Vibrio cholerae* Δ*vrrA* Δ*micV* strains carrying the indicated reporter plasmids (*x*-axis) and either an empty vector control (pCtr), the pMicV, or the pVrrA plasmid were cultivated in M9 minimal medium, and GFP fluorescence was measured. Fluorescence of the control strains was set to 1. The target genes were classified according to (B): regulated by both sRNAs (C), regulated only by MicV (D), or regulated only by VrrA (E).

Data information: In (C–E), data are presented as mean ± SD, $n = 3$.
Source data are available online for this figure.

with a second plasmid transcribing either *micV* or *vrrA* from a P_{Tac} promoter. We confirmed post-transcriptional control of 16 target mRNAs: Eight of these targets were regulated by both sRNAs, five targets were specific to MicV, and three targets were only regulated by VrrA (Fig 2C–E). Although gene expression changes obtained by RNA-sequencing were confirmed by qRT–PCR (Appendix Fig S2), we have not been able to further validate post-transcriptional control of *dsbA*, *vc1743-vc1744*, *vca0996*, *vc2240*, *vc1485*, *vc0429*, *vca0447*, *vca0845*, and *vca0789* by MicV and/or VrrA with the reporter assays (Appendix Table S2), suggesting that these genes might not be directly controlled by the sRNAs or that the relevant base-pairing sequences are lacking in the GFP reporter constructs. In agreement with our initial hypothesis, we discovered that VrrA and MicV both post-transcriptionally regulate *ompT* and that the protein products of several of the newly identified target genes are predicted to localize to the outer membrane or periplasmic space of *V. cholerae* (*e.g.,* OmpA, OmpU, Pal, Lpp, BamD, DsbD, BtuB, TolC, AcfA, and UshA). In addition, the operon encoding σ^E, the anti-sigma factor RseA, and the auxiliary regulators RseB and RseC is repressed at the post-transcriptional level by MicV and VrrA (Fig 2C, Appendix Fig S2A and Appendix Table S2). These data indicate that the σ^E response of *V. cholerae* comprises an auxiliary autoinhibitory loop that involves the base-pairing capacity of the two sRNAs.

Molecular basis for target mRNA recognition by MicV and VrrA

To understand how MicV and VrrA distinguish between shared and unique target genes, we selected three representative examples showing stable RNA duplexes (Appendix Fig S3) for further analysis: MicV-*ompT* (shared target), MicV-*ushA* (MicV-specific), and VrrA-*lpp* (VrrA-specific). We used the RNA hybrid algorithm (Rehmsmeier *et al*, 2004) to search for potential RNA duplexes formed between the sRNAs and their targets (Fig 3A–C and Appendix Fig S3A–C). For the MicV-*ompT* interaction, we predicted a 16-bp-long consecutive interaction involving the sequence of the MicV 5′ end and the ribosome binding site (RBS) of *ompT* (Fig 3A). The MicV and *ushA* RNA duplex was also predicted to involve the 5′ end of MicV; however, the interaction was shorter (10 bp) and required a sequence located upstream of the RBS in the 5′ UTR of *ushA* (Fig 3B). Interaction of VrrA and *lpp* was predicted to involve the RBS of *lpp* and a conserved sequence element located in the distal part of VrrA (nucleotides 90–107; Figs 3C and EV2A), which is separated from the sequence required to form the VrrA-*ompT* interaction (Song *et al*, 2010).

Next, we tested these predictions by mutational analysis (Figs 3D–F and EV2B). Point mutations in MicV (M1) abrogated repression of *ompT::gfp*, and conversely, mutation of *ompT* blocked target regulation by native MicV. Combination of the two dinucleotide mutations restored regulation and confirmed the predicted interaction (Fig 3A and D). The MicV M1 mutation also abrogated repression of *ushA::gfp*, which was restored by the compensatory change in the *ushA* mRNA (Fig 3E), showing that MicV uses a seed sequence located at the 5′ end of the sRNA to interact with *ompT* and *ushA*. To test the interaction between VrrA and *lpp*, we mutated three consecutive nucleotides in *vrrA* (M2, Fig 3C). Indeed, this mutation blocked repression of *lpp::gfp* and conversely mutation of the *lpp* interaction site prevented repression by native VrrA (Fig 3F). Regulation was restored and further increased when the two mutated variants were co-transformed, validating the predicted RNA duplex formation.

To study the relevance of shared versus specific base-pairing by MicV and VrrA in the context of the ESR, we introduced an inducible pBAD-*rpoE* plasmid into Δ*rpoE*, Δ*rpoE* Δ*vrrA*, Δ*rpoE* Δ*micV*, and Δ*rpoE* Δ*vrrA* Δ*micV V. cholerae*, cultivated these strains to early stationary phase (OD_{600} of 1.5), and induced the σ^E response by adding L-arabinose. We collected total RNA samples before and at several time points after σ^E induction and followed *ompT*, *ushA*, and *lpp* expression by qRT–PCR (Fig 3G–I). We also probed VrrA and MicV expression by Northern blot analysis, which validated the expected induction of these sRNAs (Fig EV2C). In all three cases, production of σ^E resulted in target mRNA repression. However, while *ompT* was inhibited by MicV or VrrA (Fig 3G), downregulation of *ushA* was significantly delayed in the absence of MicV (Fig 3H). Conversely, *lpp* repression relied on the presence of VrrA (Fig 3I). Together, our data show that MicV and VrrA both control a set of shared and specific targets, which are repressed upon activation of σ^E.

A conserved seed-pairing sequence in σ^E-dependent sRNAs

A comparison of the VrrA-*ompT* (Fig EV2D) and MicV-*ompT* (Fig 3A) RNA duplexes showed that both sRNAs sequester the RBS of *ompT*. Indeed, compensatory bp exchange experiments showed that region R1 of VrrA is required for *ompT* repression, while region R2 is dispensable (Fig EV2E). These data suggested that VrrA and MicV use similar seed-pairing domains to interact with *ompT*. An alignment of the VrrA R1 sequence with the 5′ end of MicV revealed a conserved sequence element of ten consecutive base-pairs, CRCUGCUUUU (R = purine), all of which engage in base-pairing with *ompT* (Fig 4A). In addition, the identical sequence was also found in the seed sequence of *rybB*, a σ^E-dependent sRNA conserved among enterobacteria but lacking in *V. cholerae* (Fig 4A and Papenfort *et al*, 2010). RybB acts analogous to MicV and VrrA by reducing the levels of OMP mRNAs, when the ESR is activated (Brosse & Guillier, 2018). Consequently, we hypothesized that all three sRNAs employ one conserved domain to mediate OMP repression. To test this idea, we performed three complementary experiments: First, we introduced a constitutive RybB plasmid (pRybB) into *V. cholerae* and compared OmpT production with strains carrying the VrrA plasmid, the MicV plasmid, or a vector control. In all three cases, sRNA over-expression resulted in strong OmpT repression (Fig 4B). Second, in the reciprocal experiment, we transferred the pMicV, pVrrA, or pRybB plasmids and a relevant control vector into a heterologous host, *i.e., E. coli*. We cultivated these cells to stationary phase (OD_{600} of 2.0) and investigated total protein samples using SDS–PAGE and Coomassie blue staining. For all three sRNAs, we discovered repression of OmpA and OmpC (Fig 4C), which are previously reported targets of RybB (Papenfort *et al*, 2010). Third, we tested the effect of MicV, VrrA, and RybB over-expression on the survival of *rpoE*-deficient *V. cholerae* when challenged with ethanol. In agreement with previous observations (Kovacikova & Skorupski, 2002), treatment with ethanol (3.5% final conc.) drastically reduced the CFU of Δ*rpoE V. cholerae* when compared to wild-type cells (Fig 4D). In contrast, over-expression of either of the three sRNAs strongly suppressed this phenotype, with

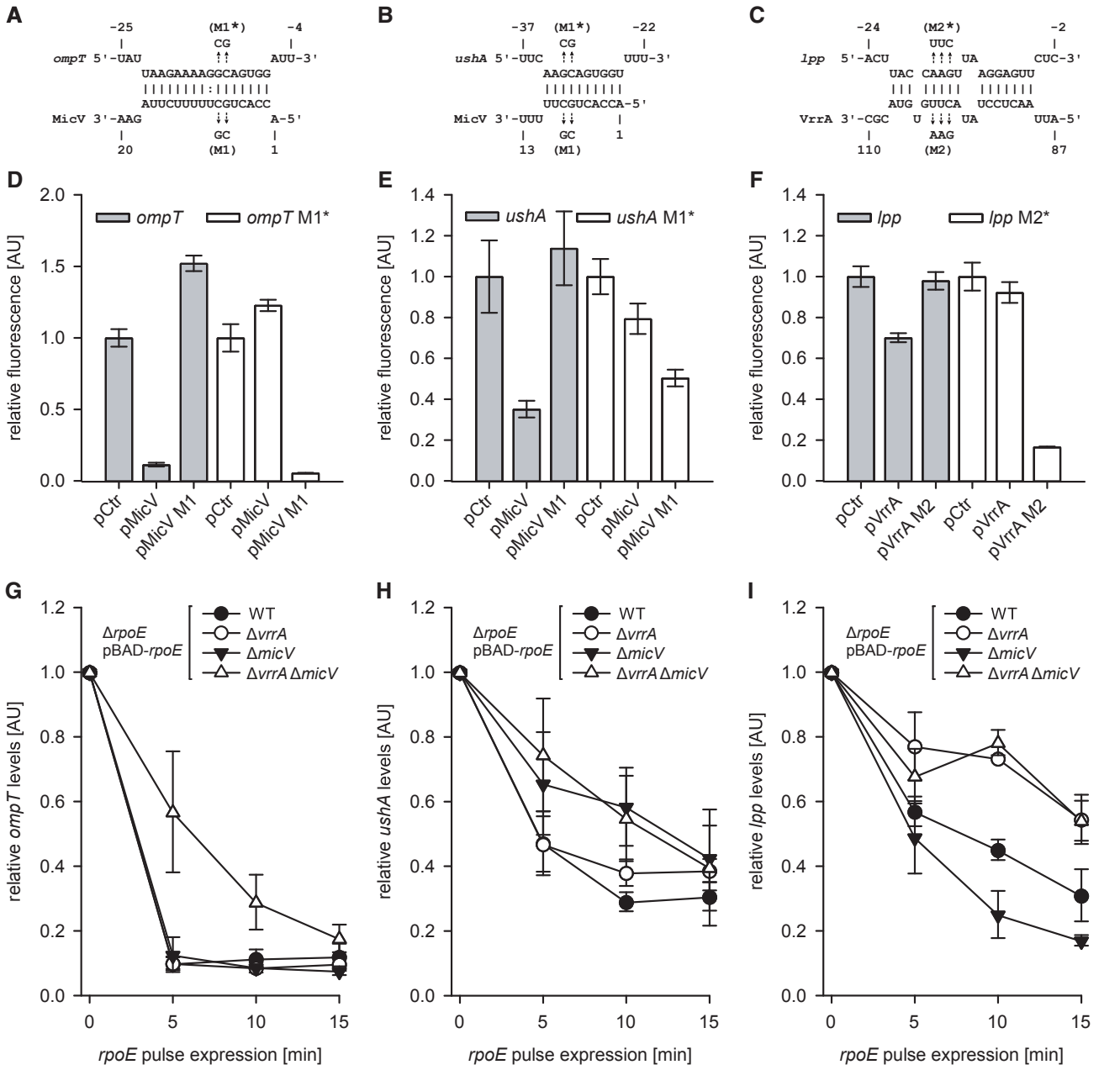

Figure 3. Patterns of target regulation by VrrA and MicV.

A–C Predicted base-pairings of MicV with the 5′UTR of *ompT* (A) and with the 5′UTR of *ushA* (B) or VrrA with the 5′UTR of *lpp* (C). Mutations tested in (D, E, F) are indicated.

D–F *Vibrio cholerae* Δ*vrrA* Δ*micV* strains carrying the *ompT*::*gfp* or *ompT* M1*::*gfp* fusions (D), *ushA*::*gfp* or *ushA* M1*::*gfp* fusions (E), or *lpp*::*gfp* or *lpp M2**::*gfp* fusions (F) and an empty vector control (pCtr), the *micV* expression plasmids (pMicV, pMicV M1), or the *vrrA* expression plasmids (pVrrA, pVrrA M2) were grown in M9 minimal medium, and GFP fluorescence was measured. M1 and M2 denote the mutations indicated in (A, B, C). Fluorescence of the control strains was set to 1.

G–I *Vibrio cholerae* Δ*rpoE*, Δ*rpoE* Δ*vrrA*, Δ*rpoE* Δ*micV*, or Δ*rpoE* Δ*vrrA* Δ*micV* strains carrying pBAD-*rpoE* or an empty vector control (pCtr) were grown in LB medium to OD_{600} of 1.5, and L-arabinose (0.2% final conc.) was added. RNA samples were collected at the indicated time points and monitored for *ompT* (G), *ushA* (H), or *lpp* (I) levels using qRT–PCR.

Data information: In (D–I), data are presented as mean ± SD, $n = 3$.
Source data are available online for this figure.

VrrA and RybB supporting cell survival ~10-fold more efficiently than MicV. These data show that, when over-expressed, σ^E-dependent sRNAs can bypass the requirement of a conditionally essential transcriptional regulator, *i.e.*, σ^E, and suggested that a conserved seed sequence present in MicV, VrrA, and RybB is responsible for this phenotype.

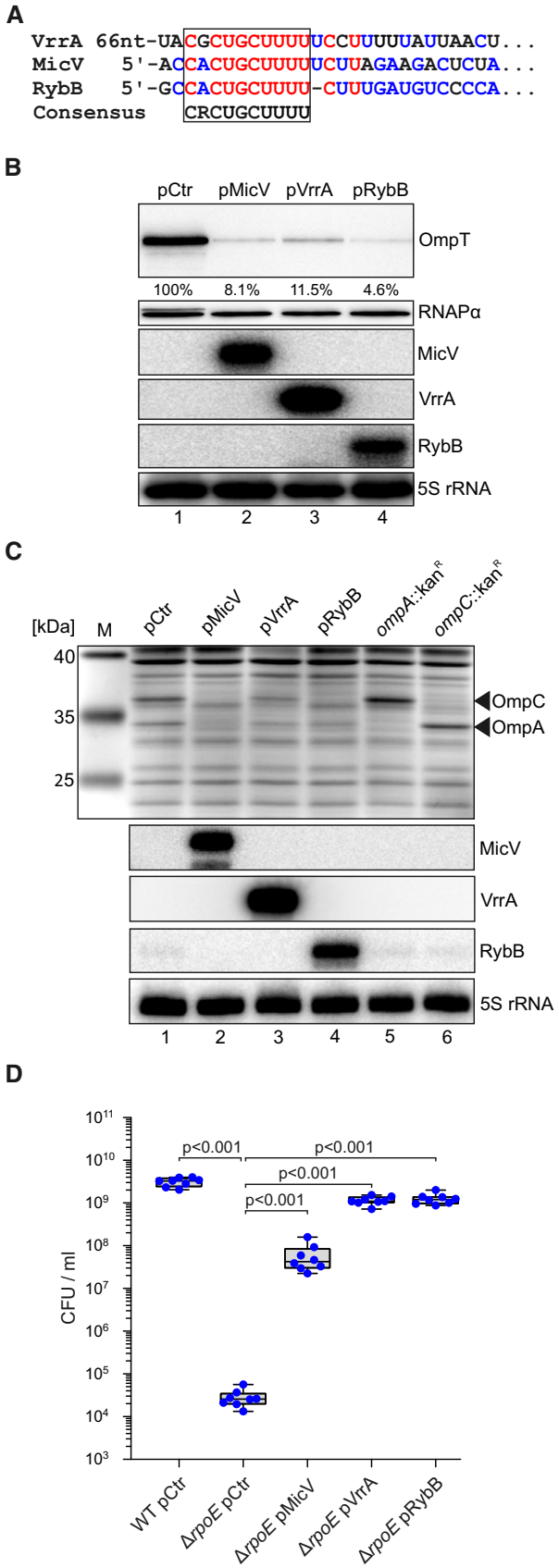

Figure 4. A conserved sRNA seed sequence inhibits OMP production.

A Alignment of the seed-pairing sequences of VrrA, MicV, and RybB.

B *Vibrio cholerae* Δ*vrrA* Δ*micV* strains carrying the *ompT*::3XFLAG gene and pMicV, pVrrA, pRybB, or an empty vector control (pCtr) were cultivated in LB medium to an OD_{600} of 2.0. RNA and protein samples were collected and analyzed for MicV, VrrA, and RybB expression on Northern blots. OmpT::3xFLAG production was tested on Western blots. RNAPα and 5S rRNA served as loading controls for Western and Northern blots, respectively.

C *Escherichia coli* wild-type strains carrying pMicV, pVrrA, pRybB, or an empty vector control (pCtr) were grown in LB medium to an OD_{600} of 2.0. RNA and protein samples were collected and investigated on Northern blots and SDS–PAGE, respectively. For comparison, we included the *E. coli* insertional mutant strains *ompA*::*kan*^{R} and *ompC*::*kan*^{R} for specific assignment of OmpA and OmpC bands.

D *Vibrio cholerae* wild-type and Δ*rpoE* strains carrying pMicV, pVrrA, pRybB, or an empty vector control (pCtr) were cultivated in LB medium to OD_{600} of 0.2 and treated with ethanol (3.5% final conc.). After 5 h of treatment, serial dilutions were prepared, recovered on agar plates, and CFU/ml were determined.

Data information: In (D), the box plots indicate the median, 75th and 25th percentiles (boxes), and 90th and 10th percentiles (whiskers), $n = 8$. Statistical significance was determined using one-way ANOVA and post hoc Holm–Sidak test. Source data are available online for this figure.

Strong enrichment for the seed-pairing sequence of σ^E-dependent sRNAs by selection experiments with randomized libraries

These results prompted us to develop an unbiased method to test the *in vivo* relevance of the conserved seed sequence present in MicV, VrrA, and RybB under stress conditions (Fig 5A). Specifically, we used the 3′ end of *E. coli* RybB, including the Hfq binding domain and the rho-independent terminator (Sauer *et al*, 2012), as a sRNA scaffold and randomized the first nine nucleotides of the seed-pairing sequence using a gene synthesis approach (see Materials and Methods for details). These constructs were cloned into a multi-copy plasmid and transferred into *V. cholerae* Δ*rpoE* cells. High-throughput sequencing of these plasmids revealed the presence of 253,570 sequence variants representing ~97% of all possible (262,144) permutations. Importantly, no single sequence variant constituted more than 0.0029% of the complete sRNA library (Fig EV3A), suggesting no major biases occurred during the construction process. Moreover, the nucleotide distribution was similar at the nine randomized positions (Fig EV3B). To select for sRNA variants providing improved stress resistance, we cultivated Δ*rpoE* cells containing the sRNA library to low cell density (OD_{600} of 0.2) and added ethanol (3.5% final conc.) to induce cell envelope stress. Following 6 h of incubation, cell dilutions were spotted on agar plates and screened for survival (Sel1; Fig 5B). Indeed, we observed a ~10-fold increase in survival of Δ*rpoE* cells carrying the sRNA library, when compared to *V. cholerae* Δ*rpoE* transformed with a control plasmid. Next, we collected the surviving cells and performed two additional rounds of selection. When compared to the Δ*rpoE* control carrying a control plasmid, survival was improved by ~1,000-fold in the second selection (Sel2) and by ~10,000-fold in the final selection (Sel3). Together, these data suggest that our approach allowed for the selection of sRNA variants providing ethanol resistance in *V. cholerae*.

To further investigate this possibility, we isolated the sRNA-containing plasmids from all three rounds of selection and

Figure 5. A conserved sRNA motif is enriched in laboratory selection experiments.

A Experimental strategy of the laboratory selection experiments: An sRNA library was generated using the *rybB* scaffold with nine randomized nucleotides at the 5′ end, cloned into a broad-range plasmid backbone, and transferred into *V. cholerae* Δ*rpoE* cells. These colonies were pooled, grown to OD_{600} of 0.2, and treated with ethanol (3.5% final conc.) for 6 h. Surviving cells were recovered on agar plates, pooled, and subjected to another round of selection (3 selections total). After each selection, the plasmids of surviving cells were analyzed using high-throughput sequencing.

B *Vibrio cholerae* wild-type and Δ*rpoE* strains carrying an empty vector control (pCtr), pRybB, or the sRNA library after consecutive selection experiments (Sel1, Sel2, and Sel3) were grown in LB medium to OD_{600} of 0.2. Cells were treated with ethanol (3.5% final conc.) for 6 h. Serial dilutions were prepared and spotted onto agar plates. R1 and R2 indicate two independent biological replicates.

C Plasmid contents of the strains carrying the sRNA libraries before selection (input) and after consecutive ethanol treatments (Sel1, Sel2, and Sel3) were analyzed using high-throughput sequencing. Relative library complexity (left *y*-axis) was determined by counting sequence variants present in the normalized samples. To test for the enrichment of possible sequence motifs, the sequence variants present in each sample were counted and normalized for sequencing depth. The resulting data were analyzed for the enrichment of the conserved CRCUGCUUUU motif (right *y*-axis).

Data information: In (C), data are presented as mean ± SD, $n = 2$.
Source data are available online for this figure.

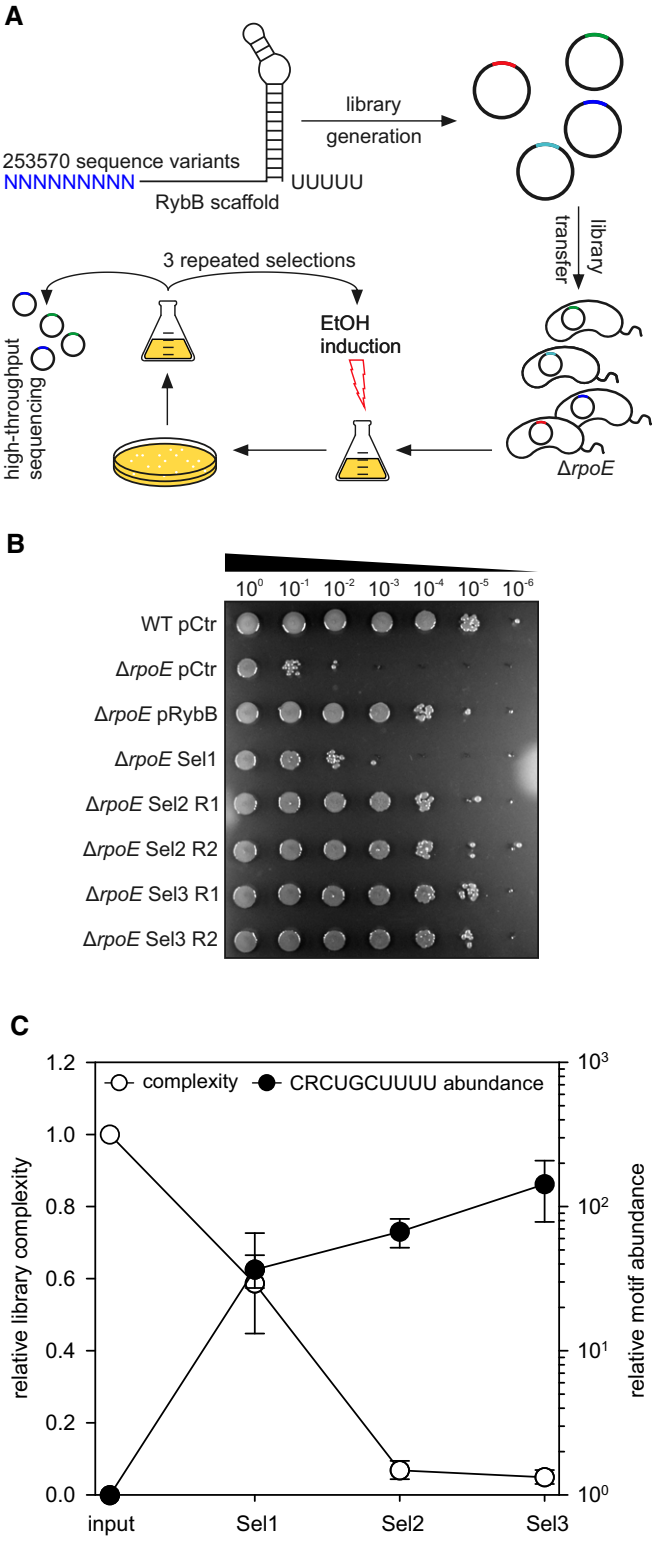

determined the number of detectable sRNA sequence variants in two biological replicates using high-throughput sequencing. After the first round of selection, the number of detected sequence variants dropped by ~40% relative to the initial sRNA library and was further reduced to ~7% and ~5% in the following two selection steps, respectively (Fig 5C). We note that the steep drop in library complexity from the first to the second selection step coincided with a substantial increase in cell survival (compare Fig 5B and C). At the same time, we also discovered a very strong enrichment (~140-fold) of the conserved seed-pairing domain present in the MicV, VrrA, and RybB sRNAs (Figs 4A and 5C; for more details on enriched variants, see below and Figs EV4 and EV5), further documenting that this motif provides protection from ethanol-induced membrane damage in *V. cholerae*.

OmpA repression mediates ethanol resistance in *Vibrio cholerae*

To investigate the molecular basis of sRNA-mediated ethanol resistance in *V. cholerae*, we hypothesized that, analogous to the native RybB, VrrA, and MicV sRNAs, the selected sRNA variants could act by modulating the accumulation of OMPs in *V. cholerae*. To test this idea, we cultivated the initial and selected sRNA libraries in LB medium to stationary phase (OD_{600} of 2.0) and isolated membrane fractions to monitor OMP production (Fig 6A). We discovered a significant decrease in the abundance of two bands in the selected sRNA libraries (lanes 5–7), when compared to the initial library (lane 4). Similarly, over-expression of the RybB sRNA, which we have shown to mediate ethanol resistance (Fig 4D), also reduced these two bands (lane 3), and mutation of Δ*rpoE* resulted in increased protein levels when compared to a wild-type control (compare lanes 1 and 2). Using mass spectrometry, we determined that both bands corresponded to OmpA, which is detectable as a premature and mature variant (Freudl *et al*, 1986). We also discovered that the abundances of OmpT and OmpU, which are targets of MicV and VrrA (Fig 2C and D), did not change during these experiments. Similarly, qRT–PCR analysis of total RNA isolated during the selection process revealed that the selected sRNAs specifically repressed *ompA*, while the mRNA levels of additional MicV/VrrA targets encoding major OMPs (*ompT*, *lpp*, *pal*, and

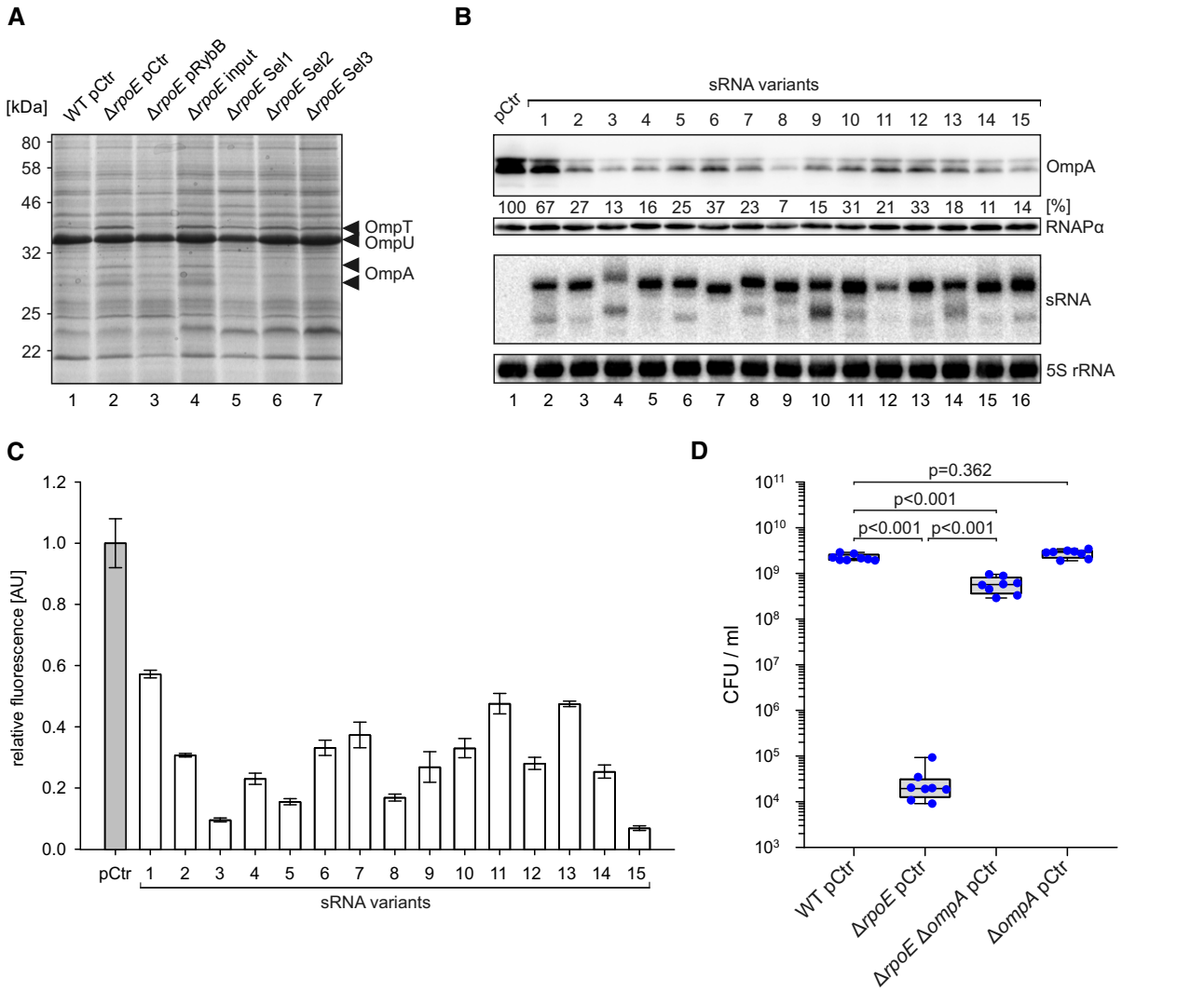

Figure 6. Enriched sRNA variants mediate ethanol resistance by OmpA repression.

A *Vibrio cholerae* wild-type and Δ*rpoE* strains carrying an empty vector control (pCtr), pRybB, or the sRNA library before (input) or after consecutive ethanol selection experiments (Sel1, Sel2, and Sel3) were cultivated in LB medium to OD_{600} of 2.0. Membrane fractions were identified by SDS–PAGE. The indicated bands were identified by mass spectrometry.

B *Vibrio cholerae* Δ*urrA* Δ*micV* cells expressing the *ompA*::3xFLAG gene and carrying an empty vector control (pCtr), or plasmids producing the 15 most highly enriched sRNA variants (sRNA variants 1–15) were grown in LB medium to an OD_{600} of 2.0. RNA and protein samples were collected and tested for sRNA and OmpA::3xFLAG expression on Northern and Western blots, respectively (with 5S rRNA and RNAPα as loading controls).

C *Vibrio cholerae* Δ*urrA* Δ*micV* strains carrying the *ompA*::*gfp* fusion and an empty vector control (pCtr) or the enriched sRNA expression plasmids were grown in M9 minimal medium, and GFP fluorescence was measured. Fluorescence of the control strains was set to 1.

D *Vibrio cholerae* wild-type, Δ*rpoE*, Δ*ompA*, or Δ*rpoE* Δ*ompA* strains were grown in LB medium to OD_{600} of 0.2 and treated with ethanol (3.5% final conc.). After 5 h of treatment, serial dilutions were prepared, recovered on agar plates, and CFU/ml were determined.

Data information: In (C), data are presented as mean ± SD, $n = 3$. In (D), the box plots indicate the median, 75th and 25th percentiles (boxes), and 90th and 10th percentiles (whiskers), $n = 8$. Statistical significance was determined using one-way ANOVA and post hoc Holm–Sidak test.
Source data are available online for this figure.

ompU) remained unchanged (Fig EV4A), suggesting that OmpA repression could be key for ethanol resistance in *V. cholerae*. To explore this possible link, we focused on the 15 most abundant sRNA variants obtained from our final round of selection (Sel3, Figs 5B and EV4B). These top 15 sRNA variants constituted ~54% of all detected sequence variants in the final selection (Fig EV4B) and were strongly enriched during the selection process (Fig EV4C). To confirm the regulatory capacity of these sRNA variants, we isolated all 15 plasmids, transformed them into independent *V. cholerae* Δ*rpoE* cells, and tested for ethanol resistance. In all 15 cases, the presence of the sRNA-expressing plasmid promoted survival (Fig EV4D). In contrast, a plasmid expressing only the *rybB* sRNA scaffold failed to restore ethanol resistance (Fig EV4D).

Next, we investigated the effect of the top 15 sRNAs on OmpA production. To this end, we added a 3XFLAG epitope to the chromosomal *ompA* locus of *V. cholerae* and transformed this strain with

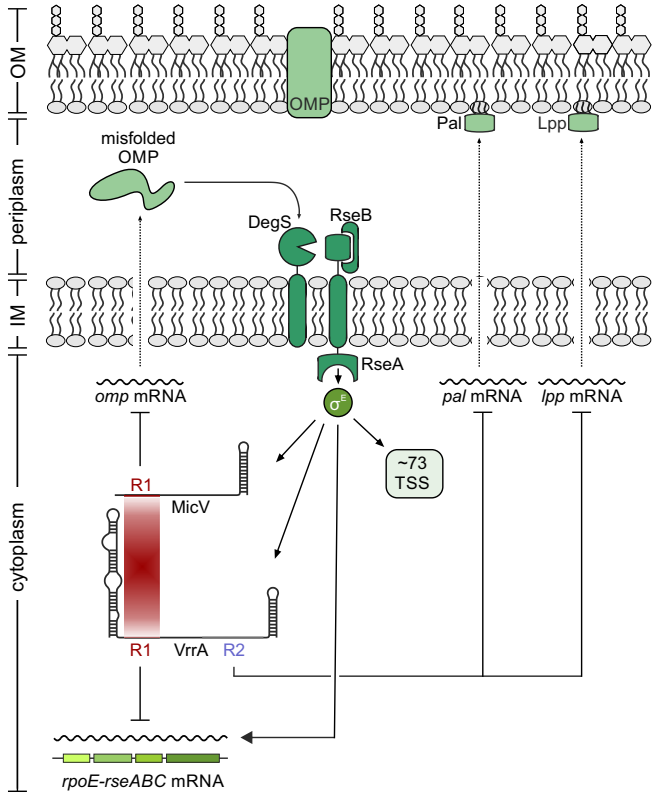

Figure 7. Conserved seed sequences control envelope homeostasis in *V. cholerae*.

Misfolded OMPs activate an intra-membrane proteolysis cascade resulting in the release of σ^E from its anti-σ factor RseA. Free σ^E activates the the expression of at least 73 transcripts in *V. cholerae*, including the *rpoE-rseABC* operon and the MicV and VrrA sRNAs. MicV and VrrA employ the conserved base-pairing region R1 to repress *omp* mRNAs, restoring membrane homeostasis, and the *rpoE-rseABC* operon. VrrA specifically downregulates *pal* and *lpp*, encoding two major lipoproteins, via the base-pairing region R2.

each of the 15 sRNA-expressing plasmids. We cultivated these cells to stationary phase (OD_{600} of 2.0) and monitored OmpA levels by Western blot (Fig 6B). For all 15 sRNA variants, we discovered significantly reduced OmpA production. However, the efficiency of the sRNA variants differed considerably with sRNA variant #1 providing only modest inhibition (~1.5-fold) and variant #8 showing the strongest repression (~14-fold), when compared to the control. All sRNA variants could be detected by Northern blot analysis indicating that the *rybB* 3′ end provides a stable sRNA scaffold (Fig 6B). To corroborate these results with a potential post-transcriptional regulatory mechanism exerted by the sRNA variants, we generated a *ompA::gfp* translational reporter whose transcription is driven by the constitutive P_{TetO} promoter. Co-transformation of this reporter with the plasmids expressing the sRNA variants into *V. cholerae* followed by GFP measurements revealed that all 15 sRNAs inhibited OmpA::GFP production (Fig 6C). Overall, the degree of OmpA protein repression observed in *V. cholerae* (Fig 6B) matched the results of the *ompA::gfp* reporter (Fig 6C), suggesting that OmpA repression by the sRNA variants occurs predominantly at the post-transcriptional level.

Our results indicated elevated OmpA levels as a possible cause of the increased ethanol sensitivity of *V. cholerae* Δ*rpoE* cells (Fig 6A–C). To test this possibility, we deleted the *ompA* gene in wild-type and Δ*rpoE V. cholerae* and assayed ethanol resistance. In line with our previous observation (Fig 4D), *V. cholerae* lacking *rpoE* displayed strongly reduced ethanol resistance, when compared to wild-type cells (Fig 6D). In contrast, cells deficient for *rpoE* and *ompA* exhibited ~10,000-fold improved survival when challenged with ethanol, whereas *V. cholerae* wild-type and Δ*ompA* strains showed highly similar survival numbers (Fig 6D). Taken together, our screen using synthetic sRNAs pinpointed OmpA repression as a key factor for ethanol tolerance in *V. cholerae* and provided evidence that regulation at the post-transcriptional level is a crucial for this phenotype.

Discussion

A main form of transcriptional regulation in bacteria occurs through the exchange of the primary sigma factor subunit of RNA polymerase with alternative sigma factors, which direct the complex to specific promoter sequences. In sharp contrast to σ^{70}, which recognizes the majority of promoters in enterobacterial cells, promoter recognition by extracytoplasmic function σ factors (ECFs) is highly stringent, which restricts the number of target promoters, allowing ECFs to mediate very specific responses (Campagne *et al*, 2015). In *E. coli*, σ^E has been reported to control 89 unique transcription units, which typically function to safeguard the synthesis and homeostasis of the outer membrane and its protein components (Rhodius *et al*, 2006). Here, we identified 73 potential σ^E-controlled TSSs in *V. cholerae* (Appendix Table S1), one of which is responsible for driving *micV* expression (Fig 1).

Three key signals have been suggested to modulate the activity of σ^E. First, σ^E responds to misfolded OMPs activating DegS-mediated cleavage of the anti-sigma factor, RseA, which results in the release of σ^E into the cytoplasm (Mecsas *et al*, 1993). Second, periplasmic lipopolysaccharide intermediates can disassemble the RseA-RseB complex and facilitate proteolytic degradation of RseA (Lima *et al*, 2013). Third, σ^E activity is also activated by limited nutrient availability, which is caused by the production of the alarmone ppGpp and its cofactor DksA (Costanzo *et al*, 2008). In all three cases, activation of σ^E results in the transcription of the *rpoE-rseA-rseB-rseC* operon; however, only conditions supporting continuous degradation of RseA will amplify the response (Chaba *et al*, 2007). Our data suggest the existence of an additional autoregulatory loop controlling the *rpoE-rseA-rseB-rseC* operon. In contrast to the activating function of σ^E on the *rpoE* promoter, MicV and VrrA both base-pair with and reduce the production of *rpoE* (Figs 2C and 7, and Appendix Figs S2A and S3A). σ^E-dependent sRNAs were previously reported to limit σ^E activation; however, in this case the underlying mechanism was associated with the inhibitory effect of these sRNAs on OMP production (Papenfort *et al*, 2006; Thompson *et al*, 2007). Direct repression of *rpoE* by MicV and VrrA could add an additional layer of autorepression, which is independent from the status of OMP synthesis and assembly. Recently, a global screen for base-pairing interactions of Hfq-binding sRNAs suggested that the MicL sRNA, which is also controlled by σ^E (Guo *et al*, 2014), binds to the *rpoE* mRNA in *E. coli* (Melamed *et al*, 2016).

Autorepression of their own transcriptional activator has now been reported for numerous sRNAs (Brosse & Guillier, 2018), and it is interesting to speculate that sRNA-mediated repression of *rpoE* could be a conserved feature of σ^E regulons in various bacterial species. Of note, base-pairing of these sRNAs with the *rpoE* mRNA is not only likely to decrease σ^E levels, but could also inhibit the production of the anti-sigma factor RseA, as well as RseB and RseC, which could further modulate the overall output of the response.

Our work also provides relevant insights into how sRNAs evolve in the context of microbial stress response systems. For example, the *micL* gene is located in the 3′ end of the *cutC* gene of *E. coli*, and although *V. cholerae* also encodes a *cutC* homolog (*vc0730*), we did not detect significant transcription from this locus in *V. cholerae* (Papenfort *et al*, 2015). However, MicL has been shown to repress Lpp synthesis in *E. coli* (Guo *et al*, 2014), and in *V. cholerae*, this function is carried out by VrrA (Figs 2E and 7). Pal, an outer membrane component relevant for cell division and outer membrane integrity (Gerding *et al*, 2007), is repressed by MicA in *E. coli* (Gogol *et al*, 2011) and reduced by VrrA in *V. cholerae*. Finally, OmpA is inhibited by MicA and RybB in *E. coli* and *Salmonella* (Rasmussen *et al*, 2005; Udekwu *et al*, 2005; Papenfort *et al*, 2010) and repressed by VrrA and MicV in *V. cholerae* (Figs 2C and 7). These data suggest that σ^E-dependent sRNAs act as functional analogs, similar to what has been proposed for the widespread group of RyhB-like sRNAs controlling bacterial iron homeostasis (Salvail & Masse, 2012). It also indicates that the establishment of an sRNA–target mRNA interaction is a dynamic process that is driven by the physiological constraints of the overarching physiological pathways (Updegrove *et al*, 2015). In other words, sRNA-mediated repression of major OMPs, such as Lpp, Pal, and OmpA, might be crucial for a fully functional σ^E response and regulation can be achieved by various different base-pairing interactions. Indeed, sequence comparison of the *lpp*, *pal*, and *ompA* base-pairing sites in *V. cholerae* (Fig 3 and Appendix Fig S3) and *E. coli* (Gogol *et al*, 2011; Guo *et al*, 2014) showed that these are not conserved among the two organisms.

Another question pertinent to the evolution of sRNAs and their targets is why certain mRNAs are controlled by two sRNAs, while others only require one. This is particularly interesting for sRNAs which are activated by the same transcription factor, such as RybB and MicA, or MicV and VrrA. Studies in *E. coli* have shown that RybB and MicA share repression of *lamB*, *ompA*, *ompW*, *tsx*, *htrG*, and *yfeX* (Gogol *et al*, 2011), whereas MicV and VrrA both regulate *ompT*, *vca0951*, *rpoE*, *vc1563*, *dsbD*, *vc1485*, *ompA*, and *bamD* (Fig 2C). In fact, the total number of potentially co-regulated MicV/VrrA targets is significantly higher (23; Fig 2B) given that several of these targets are organized in larger operons (Appendix Fig S2). One possible explanation could be that these mRNAs accumulate to high copy numbers in the cell and that rapid repression requires the action of two sRNA regulators. In addition, differences in sRNA stabilities (Fig EV1D) and potency in target regulation (*e.g.,* due to the accessibility of relevant base-pairing sequences) could add to the picture. However, following the decay of the *ompT* mRNA upon σ^E activation, we observed that either VrrA or MicV sufficiently reduced cellular *ompT* levels (Fig 3G). Despite this redundancy in regulation, certain targets are more efficiently regulated by one of the sRNAs. For example, mutation of *micV* resulted in significantly higher OmpT levels, which remained unchanged in cells lacking *vrrA* (Appendix Fig S1B). A potential division of labor among VrrA and MicV is also supported by our phenotypic observations. Laboratory selection experiments suggested that repression of OmpA is key for ethanol resistance of *rpoE*-deficient cells (Fig 6), and although both MicV and VrrA repress *ompA* (Fig 2C), only cells lacking *vrrA* or both *vrrA* and *micV* display a significant reduction in survival upon ethanol exposure (Fig 1F). Therefore, it is likely that VrrA is most relevant in ethanol-stressed cells, while MicV is the more dominant regulator under standard growth conditions, as evident from increased σ^E activity in Δ*micV* relative to wild-type and Δ*vrrA* cells (Appendix Fig S1C). Therefore, one might speculate that MicV and VrrA act as part of the global σ^E regulon to provide protection against specific stress conditions, *e.g.,* ethanol stress.

Detailed analyses of the sequences involved in base-pairing of VrrA and MicV revealed that both sRNAs share a highly conserved seed domain, which is also present in the RybB sRNA of *E. coli* and *Salmonella* (Fig 4A). The same sequence motif was also recovered in our laboratory selection experiments (Fig 5C); the exact *rybB* sequence was also among the top 15 sRNA candidates, which we tested for repression of *ompA* (#11; Fig EV5A). Inspection of the nucleotide distribution of the variable sequence in these 15 highly selected sRNAs revealed a preference for guanine and cytosine residues at the 5′ end of the sequence (Fig EV5B), which could facilitate stable seed pairing with target mRNAs (Gorski *et al*, 2017). Remarkably, all of the 15 sRNA variants selected from > 250,000 initial sequence variants inhibited OmpA production through direct base-pairing with the mRNA (Fig 6C). *In silico* prediction of the corresponding base-pairing sequences suggests that all 15 sRNAs act by blocking access of 30S ribosomes to the *ompA* mRNA (Fig EV5C), and it is also noteworthy that the majority of these sRNAs (12/15) are predicted to interact with a sequence immediately downstream of the *ompA* start codon. In fact, mutation of codons 2–5 in chromosomal *ompA* (while leaving the amino acid sequence unchanged) in Δ*rpoE* cells abrogated rescue of ethanol sensitivity by ten of the selected sRNA variants (Fig EV5C and D; sRNA variants #2 and #14 are still able to base-pair with the mutated *ompA* variant, while variants #1, #3, and #8 base-pair outside the *ompA* coding sequence). The same mutation in *ompA* is also predicted to abolish base-pairing of MicV and VrrA, and consequently, we discovered that a *V. cholerae* strain carrying this mutation displayed ~10-fold reduced ethanol resistance, when compared to the parental wild-type strain (Fig EV5E). This effect is comparable to the decreased ethanol resistance observed for the Δ*vrrA* Δ*micV* strain (Fig 1F).

Our laboratory selection experiment identified repression of OmpA as the single key factor for ethanol resistance, at least in *rpoE*-deficient cells. It would be interesting to test whether other membrane-damaging agents, such as antimicrobial peptides or related antibiotics, would result in the selection of other sRNA variants with altered target specificities. In general, we believe that our strategy of using synthetic sRNA libraries to screen complex microbial phenotypes could become a powerful genetic tool to circumvent the tedious and cost-intensive generation of gene deletion libraries.

Materials and Methods

Bacterial strains and growth conditions

All strains used in this study are listed in Appendix Table S3. Details for strain construction are provided in the

Appendix Supplementary Material and Methods section. *V. cholerae* and *E. coli* cells were grown under aerobic conditions (200 rpm, 37°C) in either LB or M9 minimal medium containing 0.4% glucose and 0.4% casamino acids (final conc.). For stationary phase cultures, samples were collected with respect to the time points when the cells reached an $OD_{600} > 2.0$, *i.e.,* 6 h and 18 h after cells reached an OD_{600} reading of 2.0. Where appropriate, media were supplemented with antibiotics at the following concentrations: 100 μg/ml ampicillin; 20 μg/ml chloramphenicol; 50 μg/ml kanamycin; 50 U/ml polymyxin B; and 5,000 μg/ml streptomycin.

Plasmids and DNA oligonucleotides

A complete list of plasmids and DNA oligonucleotides used in this study is provided in Appendix Tables S4 and S5, respectively. Details on plasmid construction are provided in the Appendix Supplementary Material and Methods section.

RNA isolation and Northern blot analysis

Total RNA was prepared and blotted as described previously (Papenfort *et al*, 2017). Membranes (GE Healthcare Amersham) were hybridized with [^{32}P]-labeled DNA oligonucleotides at 42°C or 63°C when using riboprobes. Riboprobes were generated using the MAXIscript™ T7 Transcription Kit (Thermo Fisher Scientific), according to the manufacturer's instructions. Signals were visualized using a Typhoon Phosphorimager (GE Healthcare) and quantified using GelQuant (BioChemLabSolutions).

Quantitative real-time PCR

Experiments were performed as previously described (Papenfort *et al*, 2017). Briefly, total RNA was isolated using the SV Total RNA Isolation System (Promega), according to the manufacturer's instructions. qRT–PCR was performed using the Luna Universal One-Step RT-qPCR Kit (New England BioLabs) and the MyiQ™ Single-Color Real-Time PCR Detection System (Bio-Rad). *recA* was used as a reference gene.

Transcript stability experiments

Stability of sRNAs was determined as described previously (Papenfort *et al*, 2015). Briefly, biological triplicates of *V. cholerae* wild-type (KPS-0014) and Δ*hfq* (KPS-0054) strains were grown to OD_{600} of 1.0 and transcription was terminated by addition of 250 μg/ml rifampicin. Transcript levels were probed and quantified using Northern blot analysis.

Hfq co-immunoprecipitation

Hfq co-immunoprecipitations were performed as previously described (Chao *et al*, 2012). Briefly, *V. cholerae* wild-type (KPS-0014) and *hfq::3xFLAG* tagged strains (KPS-0995) were grown in LB medium to OD_{600} of 2.0. Lysates corresponding to 50 OD_{600} units were subjected to immunoprecipitation, using monoclonal anti-FLAG antibody (Sigma, #F1804) and Protein G Sepharose (Sigma, #P6649).

RNA-Seq analysis

Biological triplicates of *V. cholerae* Δ*vrrA* Δ*micV* strains harboring the pBAD1K-Ctr, pBAD1K-*vrrA,* or pBAD1K-*micV* plasmids were grown to early stationary phase ($OD_{600} = 1.5$) in LB medium. sRNA expression was induced by addition of L-arabinose (0.2% final conc.). After 10 min of induction, cells were harvested by addition of 0.2 volumes of stop mix (95% ethanol, 5% (v/v) phenol) and snap-frozen in liquid nitrogen. Total RNA was isolated and digested with TURBO DNase (Thermo Fisher Scientific). Ribosomal RNA was depleted using Ribo-Zero kits (Epicentre) for Gram-negative bacteria, and RNA integrity was confirmed using a Bioanalyzer (Agilent). Directional cDNA libraries were prepared using the NEBNext Ultra II Directional RNA Library Prep Kit for Illumina (NEB, #E7760). The libraries were sequenced using a HiSeq 1500 System in single-read mode for 100 cycles. The read files in FASTQ format were imported into CLC Genomics Workbench v11 (Qiagen) and trimmed for quality and 3′ adaptors. Reads were mapped to the *V. cholerae* reference genome (NCBI accession numbers: NC_002505.1 and NC_002506.1) using the "RNA-Seq Analysis" tool with standard parameters. Reads mapping to annotated coding sequences were counted, normalized (CPM), and transformed (log_2). Differential expression between the conditions was tested using the "Empirical Analysis of DGE" command. Genes with a fold change ≥ 3.0 and a FDR-adjusted *P*-value ≤ 1E-8 were defined as differentially expressed.

Western blot analysis

Experiments were performed as previously described (Papenfort *et al*, 2017). If not stated otherwise, 0.05 OD/lane were separated using SDS–PAGE, stained with "Coomassie blue-silver," or transferred to PVDF membranes for Western blot analysis. 3XFLAG-tagged fusions were detected using anti-FLAG antibody (Sigma, #F1804). RNAPα served as a loading control and was detected using anti-RNAPα antibody (BioLegend, #WP003).

Preparation of membrane protein fractions

Preparation of membrane protein fractions was performed as described previously with minor modifications (Thein *et al*, 2010). Briefly, bacteria were grown to an OD_{600} of 2.0, harvested by centrifugation, and washed in buffer 1 (0.2 M Tris–HCl pH 8, 1 M sucrose, 1 mM EDTA, and 1 mg/ml lysozyme). Cells were centrifuged (200,000 *g*, 4°C, 45 min), and the resulting pellet was resuspended in buffer 2 (10 mM Tris–HCl pH 7.5, 5 mM EDTA, 0.2 mM DTT, and 0.5 mg/ml DNase). Cells were opened using a Bead Ruptor (OMNI International; 6 passes, 30-s ON, 30-s OFF, 40% amplitude, 4°C) and centrifuged to pellet unbroken cells (15,700 *g*, 4°C, 15 min). The resulting supernatants were subjected to ultra-centrifugation (300,000 *g*, 4°C, 3 h) to obtain membrane fractions.

Fluorescence measurements

Fluorescence assays to measure GFP expression were performed as described previously (Corcoran *et al*, 2012). *Vibrio cholerae* strains expressing translational GFP-based reporter fusions were grown

overnight in M9 minimal medium and resuspended in PBS. Fluorescence intensity was quantified using a Spark 10 M plate reader (Tecan). *Vibrio cholerae* strains carrying mKate2 transcriptional reporters were grown in M9 minimal medium, samples were collected at the indicated time points, and mKate2 fluorescence was measured using a Spark 10 M plate reader (Tecan). Control samples not expressing fluorescent proteins were used to subtract background fluorescence.

Generation of a synthetic sRNA library

To construct the synthetic sRNA library, a 210 bp P_L-*rybB* fragment was synthesized *in vitro* (GeneArt) with random nucleotides at positions 1–9 of *rybB*. The fragment was re-amplified with KPO-1491/1492 and cloned into the pMD30 backbone with XbaI and XhoI. Ligated plasmids were transformed into *E. coli* S17 by electroporation and plated on selection agar. Single colonies were harvested by washing the cells off the plates with sterile PBS. Two million clones were pooled to obtain eightfold coverage. The library was conjugated into *V. cholerae* Δ*rpoE lacZ::kanR* to allow for selection on kanamycin and chloramphenicol. Again, single colonies were pooled to obtain the full library, which was subsequently used as input for the selection experiments. Complexity of the obtained library was determined using high-throughput sequencing of the isolated plasmids.

sRNA library sequencing and analysis

To assess the complexity of the initial and selected RybB libraries, the plasmids were re-isolated and digested with XbaI and XhoI. The obtained P_L-*rybB* fragment was purified from agarose gels and used as input for library generation using the NEBNext Ultra II DNA Library Prep Kit for Illumina (NEB, #E7645) and sequenced using an Illumina MiSeq. The read files in FASTQ format were imported into CLC Genomics Workbench v11 (Qiagen) and trimmed to remove P_L promoter and *rybB* backbone sequences to obtain reads containing only the nine randomized nucleotides. Abundance of the individual sequences was determined using the custom python script FrequencyAnalyzer, accessible on GitHub (https://github.com/Loxos/srna-tool-kit-python). To normalize for different sequencing depths when comparing library complexity, 800,000 reads were sampled from each replicate and the number of different sequences was counted in each sample.

Ethanol stress assays

Vibrio cholerae strains were grown to exponential phase (OD_{600} of 0.2) in LB medium and challenged with ethanol (3.5% final conc.). Following 5 h of incubation, serial dilutions were prepared and recovered on agar plates to determine CFU/ml. For laboratory selection experiments, the initial Δ*rpoE* sRNA library and control strains (WT pCtr, Δ*rpoE* pCtr, and Δ*rpoE* pRybB) were grown in LB medium to exponential phase (OD_{600} of 0.2) and challenged with ethanol (3.5% final conc.). Following 6 h of incubation, cells were recovered on agar plates to test for survival. At least 1 million single clones were pooled to generate the enriched sRNA libraries, which were used as input for the next round of selection following the same protocol. High-throughput sequencing of the isolated plasmids after each selection step was used to determine library complexity and distribution of the sRNA variants.

Quantification and statistical analysis

Statistical parameters for the respective experiment are indicated in the corresponding figure legends. Details for the performed statistical tests are provided in the corresponding Source data files. Statistical analysis of CFU recovered during ethanol stress assays was performed as follows: The data were log10-transformed and tested for normality and equal variance using Kolmogorov–Smirnov and Brown–Forsythe tests, respectively. The data were tested for significant differences using one-way ANOVA and post hoc Holm–Sidak test or *t*-test. Significance levels are reported in the corresponding figure legends and Source data files. Statistical analysis was performed using SigmaStat v04 (Systat). No blinding or randomization was used in the experiments. No estimation of statistical power was used before performing the experiments, and no data were excluded from analysis.

Data and software availability

The datasets and computer code produced in this study are available in the following databases:

- RNA-Seq and NGS data: Gene Expression Omnibus (GEO) GSE125224 (https://www.ncbi.nlm.nih.gov/geo/query/acc.cgi?acc=GSE125224).
- Variant analysis computer scripts: GitHub (https://github.com/Loxos/srna-tool-kit-python).
- Motif search computer script: Zenodo (https://zenodo.org/record/2543422).

Expanded View for this article is available online.

Acknowledgements
We thank Helmut Blum, Stefan Krebs, and Andreas Brachmann for help with the RNA-sequencing experiments and Andreas Starick for excellent technical support. We also thank Dietrich H. Nies and Kirsten Jung for providing strains, Michaela Huber for help with the Hfq co-immunoprecipitation experiments, Martin Lehmann for support with the mass spectrometry analyses, and Daniel Hoyos for supplying a custom python script. We thank Jörg Vogel and Gisela Storz for comments on the manuscript and all members of the Papenfort laboratory for insightful discussions and suggestions. This work was supported by the German Research Foundation (DFG—GRK2062/1 and Exc114-2), the Human Frontier Science Program (CDA00024/2016-C), and the European Research Council (StG-758212). R.H. and K.P. acknowledge support by the Joachim Herz Foundation and Young Scholars' Programme of the Bavarian Academy of Sciences and Humanities, respectively.

Author contributions
NP, MH, RH, and KP designed the experiments; NP, MH, and RH performed the experiments; NP, MH, RH, KUF, and KP analyzed data; NP, MH, RH, and KP wrote the manuscript.

Conflict of interest
The authors declare that they have no conflict of interest.

References

Balbontin R, Fiorini F, Figueroa-Bossi N, Casadesus J, Bossi L (2010) Recognition of heptameric seed sequence underlies multi-target regulation by RybB small RNA in *Salmonella enterica*. *Mol Microbiol* 78: 380 – 394

Bouvier M, Sharma CM, Mika F, Nierhaus KH, Vogel J (2008) Small RNA binding to 5′ mRNA coding region inhibits translational initiation. *Mol Cell* 32: 827 – 837

Brosse A, Guillier M (2018) Bacterial small RNAs in mixed regulatory networks. *Microbiol Spectr* 6: RWR-0014-2017

Campagne S, Allain FH, Vorholt JA (2015) Extra Cytoplasmic Function sigma factors, recent structural insights into promoter recognition and regulation. *Curr Opin Struct Biol* 30: 71 – 78

Chaba R, Grigorova IL, Flynn JM, Baker TA, Gross CA (2007) Design principles of the proteolytic cascade governing the sigmaE-mediated envelope stress response in Escherichia coli: keys to graded, buffered, and rapid signal transduction. *Genes Dev* 21: 124 – 136

Chao Y, Papenfort K, Reinhardt R, Sharma CM, Vogel J (2012) An atlas of Hfq-bound transcripts reveals 3′ UTRs as a genomic reservoir of regulatory small RNAs. *EMBO J* 31: 4005 – 4019

Chao MC, Zhu S, Kimura S, Davis BM, Schadt EE, Fang G, Waldor MK (2015) A cytosine methyltransferase modulates the cell envelope stress response in the cholera pathogen [corrected]. *PLoS Genet* 11: e1005666

Chatterjee E, Chowdhury R (2013) Reduced virulence of the *Vibrio cholerae* fadD mutant is due to induction of the extracytoplasmic stress response. *Infect Immun* 81: 3935 – 3941

Corcoran CP, Podkaminski D, Papenfort K, Urban JH, Hinton JC, Vogel J (2012) Superfolder GFP reporters validate diverse new mRNA targets of the classic porin regulator, MicF RNA. *Mol Microbiol* 84: 428 – 445

Costanzo A, Nicoloff H, Barchinger SE, Banta AB, Gourse RL, Ades SE (2008) ppGpp and DksA likely regulate the activity of the extracytoplasmic stress factor sigmaE in Escherichia coli by both direct and indirect mechanisms. *Mol Microbiol* 67: 619 – 632

Cruz JA, Westhof E (2009) The dynamic landscapes of RNA architecture. *Cell* 136: 604 – 609

Freudl R, Schwarz H, Stierhof YD, Gamon K, Hindennach I, Henning U (1986) An outer membrane protein (OmpA) of *Escherichia coli* K-12 undergoes a conformational change during export. *J Biol Chem* 261: 11355 – 11361

Gerding MA, Ogata Y, Pecora ND, Niki H, de Boer PA (2007) The trans-envelope Tol-Pal complex is part of the cell division machinery and required for proper outer-membrane invagination during cell constriction in *E. coli*. *Mol Microbiol* 63: 1008 – 1025

Gogol EB, Rhodius VA, Papenfort K, Vogel J, Gross CA (2011) Small RNAs endow a transcriptional activator with essential repressor functions for single-tier control of a global stress regulon. *Proc Natl Acad Sci USA* 108: 12875 – 12880

Gorski SA, Vogel J, Doudna JA (2017) RNA-based recognition and targeting: sowing the seeds of specificity. *Nat Rev Mol Cell Biol* 18: 215 – 228

Guo MS, Updegrove TB, Gogol EB, Shabalina SA, Gross CA, Storz G (2014) MicL, a new sigmaE-dependent sRNA, combats envelope stress by repressing synthesis of Lpp, the major outer membrane lipoprotein. *Genes Dev* 28: 1620 – 1634

Herzog R, Peschek N, Fröhlich KS, Schumacher K, Papenfort K (2019) Three autoinducer molecules act in concert to control virulence gene expression in *Vibrio cholerae*. *Nucleic Acids Res* 47: 3171 – 3183

Hor J, Gorski SA, Vogel J (2018) Bacterial RNA biology on a genome scale. *Mol Cell* 70: 785 – 799

Johansen J, Rasmussen AA, Overgaard M, Valentin-Hansen P (2006) Conserved small non-coding RNAs that belong to the sigmaE regulon: role in down-regulation of outer membrane proteins. *J Mol Biol* 364: 1 – 8

Kavita K, de Mets F, Gottesman S (2018) New aspects of RNA-based regulation by Hfq and its partner sRNAs. *Curr Opin Microbiol* 42: 53 – 61

Kovacikova G, Skorupski K (2002) The alternative sigma factor sigma(E) plays an important role in intestinal survival and virulence in *Vibrio cholerae*. *Infect Immun* 70: 5355 – 5362

Lima S, Guo MS, Chaba R, Gross CA, Sauer RT (2013) Dual molecular signals mediate the bacterial response to outer-membrane stress. *Science* 340: 837 – 841

Mecsas J, Rouviere PE, Erickson JW, Donohue TJ, Gross CA (1993) The activity of sigma E, an *Escherichia coli* heat-inducible sigma-factor, is modulated by expression of outer membrane proteins. *Genes Dev* 7: 2618 – 2628

Melamed S, Peer A, Faigenbaum-Romm R, Gatt YE, Reiss N, Bar A, Altuvia Y, Argaman L, Margalit H (2016) Global mapping of small RNA-target interactions in bacteria. *Mol Cell* 63: 884 – 897

Papenfort K, Pfeiffer V, Mika F, Lucchini S, Hinton JC, Vogel J (2006) SigmaE-dependent small RNAs of Salmonella respond to membrane stress by accelerating global omp mRNA decay. *Mol Microbiol* 62: 1674 – 1688

Papenfort K, Bouvier M, Mika F, Sharma CM, Vogel J (2010) Evidence for an autonomous 5′ target recognition domain in an Hfq-associated small RNA. *Proc Natl Acad Sci USA* 107: 20435 – 20440

Papenfort K, Podkaminski D, Hinton JC, Vogel J (2012) The ancestral SgrS RNA discriminates horizontally acquired Salmonella mRNAs through a single G-U wobble pair. *Proc Natl Acad Sci USA* 109: E757 – E764

Papenfort K, Forstner KU, Cong JP, Sharma CM, Bassler BL (2015) Differential RNA-seq of *Vibrio cholerae* identifies the VqmR small RNA as a regulator of biofilm formation. *Proc Natl Acad Sci USA* 112: E766 – E775

Papenfort K, Silpe JE, Schramma KR, Cong JP, Seyedsayamdost MR, Bassler BL (2017) A Vibrio cholerae autoinducer-receptor pair that controls biofilm formation. *Nat Chem Biol* 13: 551 – 557

Rasmussen AA, Eriksen M, Gilany K, Udesen C, Franch T, Petersen C, Valentin-Hansen P (2005) Regulation of ompA mRNA stability: the role of a small regulatory RNA in growth phase-dependent control. *Mol Microbiol* 58: 1421 – 1429

Rehmsmeier M, Steffen P, Hochsmann M, Giegerich R (2004) Fast and effective prediction of microRNA/target duplexes. *RNA* 10: 1507 – 1517

Rhodius VA, Suh WC, Nonaka G, West J, Gross CA (2006) Conserved and variable functions of the sigmaE stress response in related genomes. *PLoS Biol* 4: e2

Sabharwal D, Song T, Papenfort K, Wai SN (2015) The VrrA sRNA controls a stationary phase survival factor Vrp of *Vibrio cholerae*. *RNA Biol* 12: 186 – 196

Salvail H, Masse E (2012) Regulating iron storage and metabolism with RNA: an overview of posttranscriptional controls of intracellular iron homeostasis. *Wiley Interdiscip Rev RNA* 3: 26 – 36

Sauer E, Schmidt S, Weichenrieder O (2012) Small RNA binding to the lateral surface of Hfq hexamers and structural rearrangements upon mRNA target recognition. *Proc Natl Acad Sci USA* 109: 9396 – 9401

Sineva E, Savkina M, Ades SE (2017) Themes and variations in gene regulation by extracytoplasmic function (ECF) sigma factors. *Curr Opin Microbiol* 36: 128 – 137

Song T, Mika F, Lindmark B, Liu Z, Schild S, Bishop A, Zhu J, Camilli A, Johansson J, Vogel J *et al* (2008) A new *Vibrio cholerae* sRNA modulates

colonization and affects release of outer membrane vesicles. *Mol Microbiol* 70: 100 – 111

Song T, Sabharwal D, Wai SN (2010) VrrA mediates Hfq-dependent regulation of OmpT synthesis in *Vibrio cholerae*. *J Mol Biol* 400: 682 – 688

Song T, Sabharwal D, Gurung JM, Cheng AT, Sjostrom AE, Yildiz FH, Uhlin BE, Wai SN (2014) Vibrio cholerae utilizes direct sRNA regulation in expression of a biofilm matrix protein. *PLoS One* 9: e101280

Sorek R, Cossart P (2010) Prokaryotic transcriptomics: a new view on regulation, physiology and pathogenicity. *Nat Rev Genet* 11: 9 – 16

Storz G, Vogel J, Wassarman KM (2011) Regulation by small RNAs in bacteria: expanding frontiers. *Mol Cell* 43: 880 – 891

Thein M, Sauer G, Paramasivam N, Grin I, Linke D (2010) Efficient subfractionation of gram-negative bacteria for proteomics studies. *J Proteome Res* 9: 6135 – 6147

Thompson KM, Rhodius VA, Gottesman S (2007) SigmaE regulates and is regulated by a small RNA in *Escherichia coli*. *J Bacteriol* 189: 4243 – 4256

Udekwu KI, Darfeuille F, Vogel J, Reimegard J, Holmqvist E, Wagner EG (2005) Hfq-dependent regulation of OmpA synthesis is mediated by an antisense RNA. *Genes Dev* 19: 2355 – 2366

Updegrove TB, Shabalina SA, Storz G (2015) How do base-pairing small RNAs evolve? *FEMS Microbiol Rev* 39: 379 – 391